Spectral Simplification in Vibrational Spectroscopy Using Doubly Vibrationally Enhanced Infrared Four Wave Mixing

Wei Zhao† and John C. Wright*

Contribution from the Department of Chemistry, University of Wisconsin, 1101 University Avenue, Madison, Wisconsin 53706

Received July 26, 1999

Abstract: A new form of vibrational spectroscopy has recently been demonstrated using three coherent sources to generate nonlinear four wave mixing (FWM). It is an optical analogue of 2D NMR. The four transitions that occur in FWM include combinations of infrared absorption and Raman transitions and result in doubly vibrationally enhanced (DOVE) four wave mixing (FWM). In this paper, we use acetonitrile in different mixtures as a model system to demonstrate the spectral selectivity that allows DOVE methods to remove the spectral congestion from vibrational spectra of complex mixtures and to discriminate against a strong water background. The selectivity results from two multiplicative vibrational enhancements and the intra- and intermolecular interactions that cause mode coupling. Since DOVE features cannot occur in the absence of mode coupling, these methods isolate the spectral features that are associated with interactions. This method promises to have important applications for probing complex biological, chemical, and environmental samples.

Introduction

Vibrational infrared (IR) and Raman spectroscopies are powerful tools for studying molecular structures and interactions. However, for complex systems their use is often hindered by spectral congestion and solvent background. Noda[1] improved the spectral selectivity by developing 2D infrared correlation spectroscopy to extract structural information on polymers and proteins.[1−3] This method is based on correlation analysis of the changes that occur in conventional infrared spectra obtained under external perturbations. Cross-peaks appear in 2D spectra for coupled vibrational modes that reflect the correlated spectral changes and identify the features associated with the interactions. The method is limited by the need to detect changes in the absorption spectrum and the loss of selectivity that occurs when multiple modes are perturbed. Hochstrasser and co-workers developed a nonlinear optical analogue of these correlation methods where a laser pump caused spectral perturbations of a particular vibrational mode.[4,5] The vibrational perturbation changes a subsequent absorption spectrum probe for the modes that were coupled to the pumped mode. This type of pump−probe spectroscopy provides selectivity in the modes that are perturbed, but it is still limited by the need to detect spectral changes.

The feasibility for a new type of vibrational spectroscopy has recently been demonstrated that can achieve selectivity using the approach shown in Figure 1.[6,7] Doubly vibrationally enhanced four wave mixing (DOVE-FWM) uses two vibrational resonances where cross-peaks can only be observed if there is coupling between the vibrational modes.[8−11] The absence of uncoupled features eliminates the need to detect changes so the cross-peaks can be directly measured in 2D spectra without the need for further data treatment. The cross-peak intensities reflect similar information to the combination and overtone bands that are usually hidden by the stronger fundamental modes in one-dimensional spectra. DOVE methods are the nonlinear vibrational analogue to 2D NMR and should possess complementary capabilities.[4−7,12−19]

In this paper, we demonstrate the selective enhancements of coupled modes where the intensity of the enhancements reflects the strength of the interactions that are responsible for the vibrational mode coupling. Since interactions are often the focus of many chemical investigations, spectroscopic measurements that can isolate the features that are associated with interactions are particularly valuable. Since many applications of traditional infrared spectroscopy are compromised by the strong absorption from water, it is also important to determine the ability of DOVE

* Address correspondence to this author.
† Current address: Department of Chemistry, University of Arkansas, 2801 South University Avenue, Little Rock, AR 72204-1099.

(1) Noda, I. *J. Am. Chem. Soc.* **1989**, *111*, 8116.
(2) Schultz, C. P.; Fabian, H.; Mantsch, H. H. *Biospectroscopy* **1998**, *4*, S19−S29.
(3) Sefara, N. L.; Magtoto, N. P.; Richardson, H. H. *Appl. Spectrosc.* **1997**, *51*, 536−540.
(4) Hamm, P.; Lim, M.; Hochstrasser, R. M. *J. Phys. Chem. B* **1998**, *102*, 6123−6138.
(5) Hamm, P.; Lim, M.; DeGrado, W. F.; Hochstrasser, R. M. *Proc. Natl. Acad. Sci.* **1999**, *96*, 2036−2041.
(6) Zhao, W.; Wright, J. C. *Phys. Rev. Lett.* **1999**, *83*, 1950−1953.
(7) Zhao, W.; Wright, J. C. *Phys. Rev. Lett.* Submitted for publication.
(8) Okumura, K.; Tanimura, Y. *J. Chem. Phys.* **1997**, *106*, 1687−1698.
(9) Cho, M. *J. Chem. Phys.* **1998**, *109*, 5327−5337.
(10) Chernyak V.; Mukamel, S. *J. Chem. Phys.* **1998**, *108*, 5812−5825.
(11) Tanimura Y.; Mukamel, S. *J. Chem. Phys.* **1993**, *99*, 9496−9511.
(12) Wright, J. C.; Chen, P. C.; Hamilton, J. P.; Zilian, A.; LaBuda, M. J. *Appl. Spectrosc.* **1997**, *51*, 949−958.
(13) Chen, P. C.; Hamilton, J. P.; M. A. Zilian,; J. J. LaBuda,; Wright, J. C. *Appl. Spectrosc.* **1998**, *52*, 380−392.
(14) Zimdars, D.; Tokmakoff, A.; Chen, S.; Greenfield, S. R.; Fayer, M. D.; Smith, T. I.; Schwettman, H. A. *Phys. Rev. Lett.* **1993**, *70*, 2718−2722.
(15) Rector, K. D.; Fayer, M. D.; Engholm, J. R.; Crosson, T. E.; Smith, I.; Schwettman, H. A. *Chem. Phys. Letts.* **1999**, *305*, 51−56.
(16) Steffen, T.; Duppen, K. *Phys. Rev. Lett.* **1996**, *76*, 1224−1227.
(17) Ulness, D. J.; Kirkwood, J. C.; Albrecht, A. C. *J. Chem. Phys.* **1998**, *108*, 3897−3902.
(18) Tokmakoff, A.; Lang, M. J.; Larsen, D. S.; Fleming, G. R.; Chernyak, V.; Mukamel, S. *Phys. Rev. Lett.* **1997**, *79*, 2702−2705.
(19) Zhang, W. M.; Chernyak, V.; Mukamel, S. *J. Chem. Phys.* **1999**, *110*, 5011−5028.

10.1021/ja9926414 CCC: $18.00
Published on Web 11/11/1999

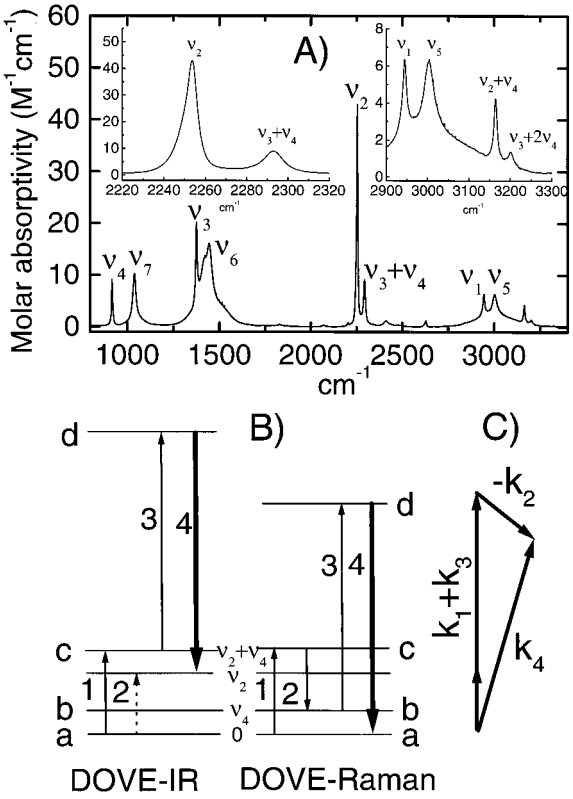

Figure 1. (A) Absorption spectra of acetonitrile including expanded regions in the spectral range used for this work. (B) Evolution of coherence for DOVE-IR and DOVE-Raman. The arrows show the transitions that cause the evolution of the DOVE-IR and DOVE-Raman coherences. The numbers label the input frequencies described in the text and the letters indicate the states described in eq 2. Solid arrows show ket evolution and dotted arrows show bra evolution for a coherence that is a linear combination of states *i* and *j*. The bold arrow denotes the output coherence. (C) Phase matching diagram for DOVE-FWM.

methods to probe aqueous solutions. We show that the DOVE methods strongly discriminate against the water absorption and narrow the broadened line caused by water. We also use the DOVE-FWM methods for a mixture of seven components and demonstrate that DOVE-FWM can isolate a coupled mode, even though the spectra are congested in both conventional infrared and Raman spectra. Our results demonstrate the feasibility and features required to make DOVE methods practical for a wide range of scientific applications where identification of intra- and intermolecular interactions is important.

Theory

Vibrational spectroscopy is based on the resonances in generating a polarization, *P*, from the oscillating electric fields, *E*, of exciting electromagnetic radiation. Nonlinearities develop in generating the polarization response when the electric fields within a sample become large so the oscillating polarization acquires distortions at new frequencies. Four wave mixing spectroscopy is based on the distortions that depend on the cube of the electric field:[12]

$$P = \chi^{(3)}E^3 \tag{1}$$

where $\chi^{(3)}$ is the third-order susceptibility. The frequency dependence of $\chi^{(3)}$ is described by:

$$\chi^{(3)} = \sum_{a,b,c,d=\text{all states}} \frac{A_1}{(\omega_{ca} - \omega_1 - i\Gamma_{ca})} + \frac{A_2}{(\omega_{ba} - \omega_2 + i\Gamma_{ba})} + \frac{A_3}{(\omega_{ca} - \omega_1 - i\Gamma_{ca})(\omega_{ba} - \omega_2 + i\Gamma_{ba})} + \frac{A_4}{(\omega_{ca} - \omega_1 - i\Gamma_{ca})(\omega_{ba} - (\omega_1 - \omega_2) - i\Gamma_{ba})} + \frac{A_5}{(\omega_{ba} - (\omega_1 - \omega_2) - i\Gamma_{ba})} + A_6 \tag{2}$$

where ω_{ij} and Γ_{ij} are the frequency difference and dephasing rates for states *i* and *j*, ω_n is the frequency of laser *n*, and A_i is a proportionality constant.[12] The labeling refers to Figure 1B. The six terms correspond to different four wave mixing processes and each has three resonances with either electronic or vibrational states.[12] However, many resonances are not important, particularly those associated with distant electronic states. Therefore, this equation shows only the vibrational resonances explicitly and the electronic resonances are combined with the constants in the numerator. The FWM output signal intensity at $\omega_4 = \omega_1 - \omega_2 + \omega_3$ is proportional to $|P|^2$ and since the expression for $|\chi^{(3)}|^2$ contains cross-terms, there are changes in the spectral line shape that are caused by the interference between the polarization waves of the different processes.

Each of the terms in eq 2 has a characteristic frequency dependence. For the experiments in this paper, we scan the ω_1 frequency for constant values of ω_2. The first two terms in the equation describe singly vibrationally enhanced (SIVE) processes caused by the infrared absorption transition at ω_1 or ω_2.[20] Term 1 produces peaks when ω_1 matches infrared absorption transitions but the peaks have no dependence on ω_2. Term 2 produces a background that maximizes when ω_2 matches infrared absorption transitions, independently of the ω_1 value. Term 3 describes the DOVE-IR-FWM process (see Figure 1B) that produces peaks when ω_1 matches absorption transitions and the peaks maximize when ω_2 match other absorption transitions. Term 4 describes the doubly vibrationally enhanced Raman-like (DOVE-Raman-FWM) process (see Figure 1B) that produces peaks when $\omega_1 - \omega_2$ match vibrational frequencies and the peaks maximize when ω_1 match an infrared absorption transition. Term 5 describes ordinary Raman processes that produce peaks when $\omega_1 - \omega_2$ match vibrational frequencies independently of the absolute ω_1 or ω_2 values. The last term describes nonresonant processes, which produce a background that is independent of ω_1 and ω_2. It is this term that determines the detection limits of nonlinear methods. The A_i contain four transition moments that control the intensity of each process. Normally, vibrational transition moments vanish if more than one vibrational quantum changes in the transition. Since a cross-peak between two modes from a DOVE term requires at least one transition with multiple quantum state changes, there must be at least one transition moment that involves anharmonicities or nonlinear polarizabilities that couple modes so transitions with multiple vibrational quanta changes occur.[7−11]

The DOVE processes can be described as two infrared transitions and a Raman transition that occur simultaneously

(20) Labuda, M. J.; Wright, J. C. *Phys. Rev. Lett.* **1997**, *79*, 2446−2450.

during the presence of the excitation beams. In the DOVE-IR process, two infrared absorption transitions occur to different vibrational states and the Raman transition occurs between the two states. Mode coupling is manifested through combination or overtone transitions in the infrared absorption transitions and/or the Raman transition. In the DOVE-Raman process, an infrared absorption and an infrared emission transition occur to different vibrational states and the Raman transition occurs between the two states. Here also, mode coupling is manifested through combination band or overtone transitions in the infrared absorption transitions and/or the Raman transition. In all cases, the combination or overtone bands require anharmoncities or nonlinear polarizabilities that reflect the intra- or intermolecular interactions that couple modes.

In this paper, we explore how the relative importance of the different terms and processes described by eq 2 affects the selectivity of DOVE-FWM methods for spectral simplification of complex mixtures. In a mixture, each component has a $\chi^{(3)}$ given by eq 2 and the overall nonlinearity is the sum of all the contributions. Acetonitrile has been observed to have a DOVE peak that is enhanced by double resonance with two modes that are coupled by intramolecular interaction, and the selectivity that characterizes the DOVE peak depends on its importance relative to the other processes.[6,7] We create a mixture where other components can have SIVE resonances in both the ω_1 and ω_2 frequency ranges as well as electronic contributions to the background. Each vibrational state in each component can potentially contribute both when it is resonant with one or more frequencies and when it is nonresonant since eq 2 shows the nonlinearity depends on a sum over all states. Experimentally, the central question that must be answered to define the selectivity of DOVE methods is the extent to which the DOVE contributions in eq 2 dominate over the other competing contributions from all the states and components in the mixture.

Experimental Section

This work involved the use of three samples: an acetonitrile (97 mol %)/deuteriobenzene (3 mol %) solution, an acetonitrile (40 mol %)/water (60 mol %) solution, and a seven-component mixture composed of acetonitrile (CH_3CN), deuterated acetonitrile (CD_3CN), deuterated chloroform ($CDCl_3$), tetrahydrofuran (THF, C_4H_8O), deuterated C_4D_8O (THF-d_8), deuterated benzene (C_6D_6), and distilled water (H_2O). All components have a volume ratio of one relative to acetonitrile except C_6D_6 and water. C_6D_6 has a volume ratio 0.15 and water has a value of 0.25, respectively. All chemicals are from Aldrich with purity >99%.

The FWM experiments use an injection seeded Nd:YAG laser (Coherent, Inc.) to pump two optical parametric oscillators/amplifiers (OPO/OPA) (LaserVision, WA) that generate two tunable IR laser beams at ω_1 and ω_2 and frequencies that are tunable from the near-IR to $\approx$2150 cm^{-1} with bandwidths of $\approx$3−5 cm^{-1}. The 532 nm Nd:YAG output provides the ω_3 beam and the output beam at $\omega_4 = \omega_1 - \omega_2 + \omega_3$ is monitored with filters and a photomultiplier. All the beams are linearly polarized in identical directions. The ω_1 and ω_3 beams are collinear and the ω_2 beam crosses them at an angle between 10 and 20° to provide phase matching (Figure 1C). The sample holder is a borosilicate rectangular capillary with a path length of 100 μm.

The deuteriobenzene in the samples provides a convenient internal standard because the $\omega_1 - \omega_2 = 944$ cm^{-1} Raman ring breathing mode has a well-known value for the third-order susceptibility, $\chi^{(3)}$. Figure 2A shows the acetonitrile absorption spectrum.[21] The important CH_3CN modes for this work are the strong C≡N stretch absorption at 2253 cm^{-1} (ν_2), the C−H bend at 1372 cm^{-1} (ν_3), a C−C stretch Raman band at 918 cm^{-1} (ν_4), C−H stretch absorptions at 2944 and 3003 cm^{-1} (ν_1 and ν_5), and three combination bands at 2293, 3164, and 3200 cm^{-1} corresponding to ($\nu_3 + \nu_4$), ($\nu_2 + \nu_4$), and ($\nu_3 + 2\nu_4$), respectively.[22,23] Our experiments fix ω_2 at different positions near the C≡N stretch and scan ω_1 across the 2900−3300 cm^{-1} region.

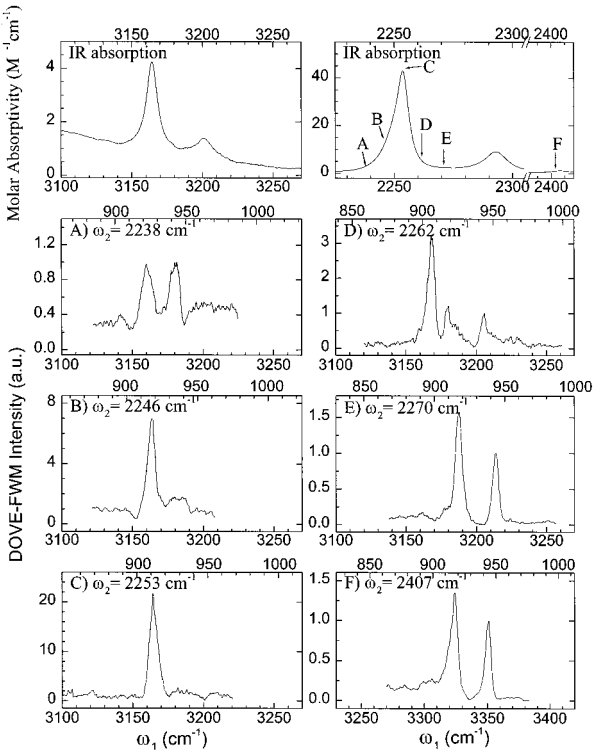

Figure 2. The top two spectra show the absorption bands in the region of the ω_1 and ω_2 values used for the DOVE-FWM experiments. The lower spectra show FWM spectra where ω_1 is scanned while ω_2 is set at the indicated positions. The ω_2 positions are also indicated by letters in the absorption spectrum to show their relationship to the absorption spectrum for the different scans. The FWM spectra have two abscissa showing ω_1 (bottom axis) and $\omega_1 - \omega_2$ (top axis) so Raman and infrared resonances can be identified more easily. The sample is a 97% acetonitrile, 3% deuteriobenzene mixture.

Results

Acetonitrile is an appropriate model system for exploring the characteristics of DOVE-FWM because there is a well-defined $\nu_2 + \nu_4$ combination band associated with mode coupling between ν_2 and ν_4. The mode coupling occurs because vibrational excitation of the C≡N bond modulates the electron density associated with the C−C bond. DOVE-IR-FWM can then probe the coupling by using the $0 \rightarrow \nu_2$ and $\nu_2 + \nu_4$ absorption transitions and the $\nu_2 + \nu_4 \rightarrow \nu_2$ Raman transition for the FWM process. All the transitions involve single vibrational quantum changes except for the $0 \rightarrow \nu_2 + \nu_4$ two quanta transition of the combination band that provides the connection between the ν_2 and ν_4 modes.

Figure 2 shows the FWM spectra of CH_3CN with 3 mol % C_6D_6 as ω_1 is scanned and ω_2 is set at the frequencies listed above each spectrum. The figure also shows the absorption spectra in the region of the ω_1 and ω_2 frequencies. The absorption spectra have the $\nu_2 + \nu_4$ and $\nu_3 + 2\nu_4$ combination bands at $\omega_1 = 3164$ and 3200 cm^{-1}, respectively, the ν_2 fundamental at $\omega_2 = 2253$ cm^{-1}, and the $\nu_3 + \nu_4$ combination band at $\omega_2 = 2293$ cm^{-1}. The FWM spectra contain a line at $\omega_1 - \omega_2 = 944$ cm^{-1} from the deuteriobenzene internal standard

(21) Bertie, J. E.; Lan, Z. *J. Phys. Chem. B* **1997**, *101*, 4111−4119.

(22) Deak, J. C.; Iwaki, L. K.; Dlott, D. D. *J. Phys. Chem. A* **1998**, *102*, 8193−8201.

(23) Venkateswarlu, P. *J. Chem. Phys.* **1951**, *19*, 293−298.

that serves as an intensity reference since its contribution always reflects the same $\chi^{(3)}$ value, independent of the ω_2 value. When ω_2 is detuned from the 2253 cm^{-1} ν_2 mode, two lines appear in the spectrum from the $\omega_1 - \omega_2 = 918$ and 944 cm^{-1} Raman lines of acetonitrile and deuteriobenzene, respectively. These lines are clearly seen in the spectra for $\omega_2 = 2238$, 2270, and 2407 cm^{-1}. The letters in the absorption spectrum show the positions of ω_2 relative to the strong absorption peaks. Note that the 2407 cm^{-1} spectrum is obtained at an ω_2 value that is far from any significant absorption feature so the spectrum reflects the relative intensity ratio expected for the two Raman peaks. Since the lines in the $\omega_2 = 2238$ and 2270 cm^{-1} have the same intensity ratio as the spectrum with $\omega_2 = 2407$ cm^{-1}, there is no significant contribution from DOVE processes at these frequencies. However, when ω_2 is tuned to 2246 cm^{-1}, there is appreciable absorption from the ν_2 mode and a large peak appears at $\omega_1 = 3164$ cm^{-1}. The deuteriobenzene Raman line at $\omega_1 - \omega_2 = 944$ cm^{-1} has become insignificant relative to this line because of the large enhancement. This ω_1 frequency matches the $\nu_2 + \nu_4$ absorption band so there are strong DOVE enhancements from both the DOVE-Raman process where ω_1 is resonant with the $0 \rightarrow \nu_2 + \nu_4$ transition while ω_2 is resonant with the $\nu_2 + \nu_4 \rightarrow \nu_2$ transition and the DOVE-IR process where ω_1 is resonant with the $0 \rightarrow \nu_2 + \nu_4$ transition while ω_2 is near resonance with the $0 \rightarrow \nu_2$ transition. The peak becomes even larger in the spectrum with $\omega_2 = 2253$ cm^{-1} because the DOVE-IR process is fully resonant. Here, ω_1 matches the $0 \rightarrow \nu_2 + \nu_4$ transition and ω_2 matches the $0 \rightarrow \nu_2$ transition. The peak diminishes when $\omega_2 = 2262$ cm^{-1} as the excitation frequency is now above the $0 \rightarrow \nu_2$ transition and the acetonitrile and deuteriobenzene Raman lines appear again at $\omega_1 - \omega_2 = 918$ and 944 cm^{-1}. The peak cannot be seen at all when $\omega_2 = 2270$ cm^{-1} and only the two Raman lines are seen.

It should be noted that many lines in the FWM spectra do not have symmetrical line shapes. Dispersive shapes can occur when there are two contributions to the output.[6,12] Each contribution adds additional terms to eq 2 and consequently there are more cross-terms in $|P|^2$. The cross-terms represent interference effects that change the line shapes. In the spectra, the interference occurs between the peak and the background.

We have also taken spectra in the 2900−3120 cm^{-1} region with $\omega_2 = 2253$ cm^{-1} to observe DOVE processes involving the C−H stretch modes. We did not observe any measurable DOVE peaks from the ν_1 or ν_5 modes in this region, despite the strength of the C−H absorption lines. The absence of the C−H DOVE cross-peaks reflects the absence of interactions associated with anharmonic or nonlinear polarizabilities that could lead to coupling between ν_2 and either ν_1 or ν_5 and it illustrates the strong selectivity of DOVE methods for modes that are associated with interactions. Excitation of the C≡N bond does not cause appreciable modulation of the electron density in the C−H bond. The absence of coupling between these modes is also in agreement with the results of Deak et al.[22]

Infrared absorption spectroscopy is often compromised by strong absorption from the solvent, particularly in biological systems where water provides strong absorption. It is common to use very thin sample path lengths and background subtraction techniques to extract the features that reflect molecular structure in 2D IR correlation spectroscopy.[2] Baseline fluctuations and random noise must be eliminated to avoid introducing artificial features in the 2D spectrum.[24] If DOVE methods are to be used in biological samples, it is important to discriminate against background absorption without requiring data treatment.

(24) Czarnecki, M. A. *Appl. Spectrosc.* **1998**, *52*, 1583−1590.

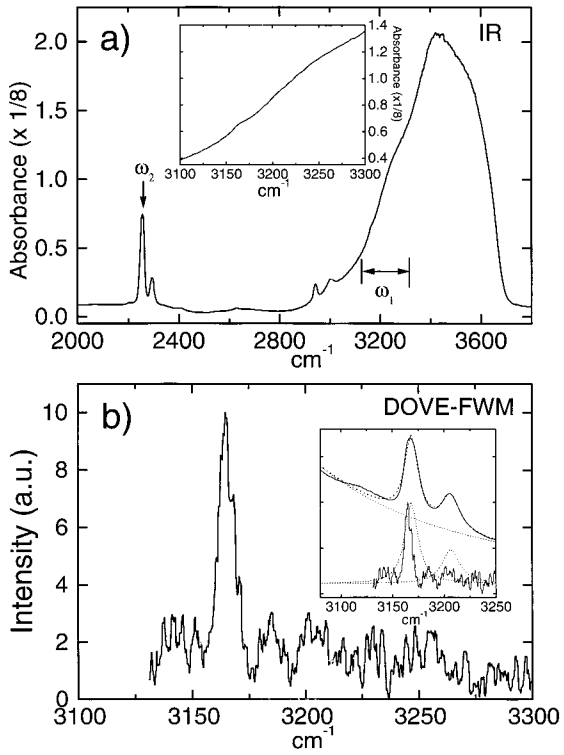

Figure 3. (a) The IR absorption spectrum and an expanded view (the inset) for a 40:60 mol % CH_3CN-H_2O solution.(b) Spectral scan of ω_1 with ω_2 at the 2253 cm^{-1} C≡N resonance. The inset shows the line narrowing of DOVE-FWM in comparison with the line width of the IR band. The upper solid line is the IR absorption spectrum obtained from a 40:60 mol % CH_3CN-D_2O solution. Dashed lines are decomposed from the solid line by using least-squares fitting. The $\nu_2 + \nu_4$ combination band of CH_3CN is broadened to 14 cm^{-1} (fwhh) with a frequency shift to 3167 cm^{-1}.

To test the sensitivity of DOVE methods to background water absorption, we applied DOVE methods to an aqueous acetonitrile sample. Figure 3 shows the spectrum of the 40:60 mol ratio CH_3CN-H_2O sample with $\omega_2 = 2253$ cm^{-1} in comparison with the absorption spectra. The absorption spectrum shows that the H_2O obscures the CH_3CN combination band at 3164 cm^{-1}. Although the absorbance in the sample exceeds 5, the DOVE-FWM spectrum contains only a single line with the same line shape as the pure material. The presence of the water does lower the absolute intensity at the peak substantially because the strong absorption limits the path length over which the FWM can occur but we still do not observe any FWM contribution from the much stronger water absorption. We attribute the weak water nonlinearity to the low Raman scattering cross-section and the large detuning of the electronic resonances from the high-energy electronic states. The strong discrimination against the water contribution suggests that DOVE methods can be used for the aqueous environments required for biological and environmental applications.

We also observe that the 3164 cm^{-1} CH_3CN DOVE-IR-FWM peak is appreciably narrower than the corresponding absorption peak. Water broadens the ν_2 C≡N stretch band and shifts its frequency to the blue, but the 3164 cm^{-1} combination band cannot be distinguished from the strong O−H stretch absorption of water. To observe water's perturbation of the 3164 cm^{-1} combination band, the infrared spectrum of an acetonitrile/deuterated water (CH_3CN/D_2O) sample was measured and is shown in the upper part of the inset in Figure 3b. The lower curve in the inset shows a comparison between the DOVE-IR

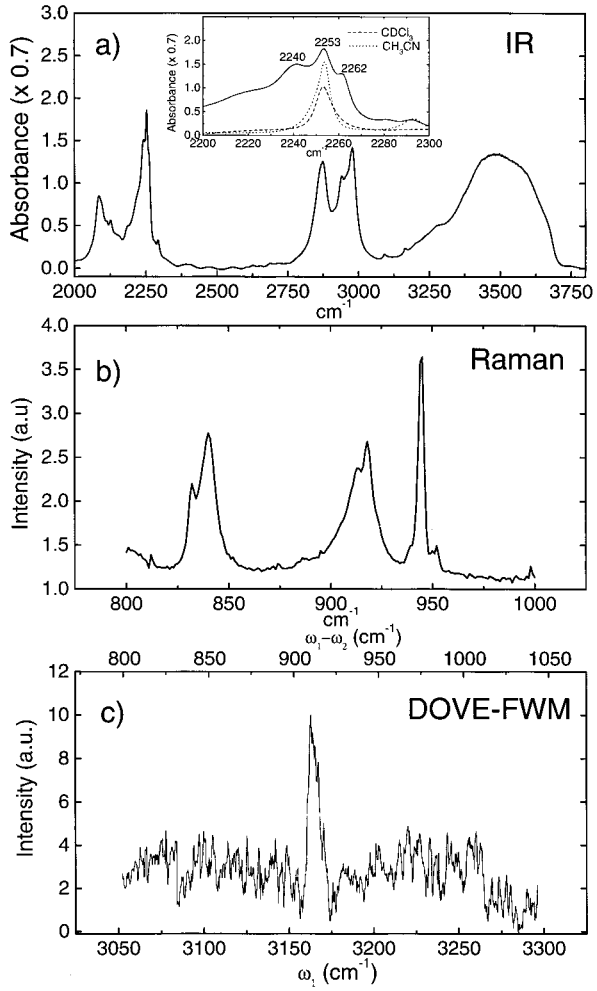

Figure 4. (a) The infrared absorption spectrum of a $CH_3CN/CD_3CN/CDCl_3/THF/THF\text{-}d_8/C_6D_6/H_2O$ mixture. The inset shows the spectral overlap near 2253 cm^{-1}. (b) Spontaneous Raman spectrum of the mixture under Ar^+ laser 514.5 nm excitation. (c) FWM spectrum of the mixture where ω_1 is scanned while ω_2 is set at the 2253 cm^{-1} C≡N resonance of CH_3CN. The bottom axis shows ω_1 and the top axis shows $\omega_1 - \omega_2$.

feature and the two absorption lines in the CH_3CN/D_2O. The water broadens and blue-shifts the $\nu_2 + \nu_4$ combination band. Previous work attributes the broadening and shifting to the presence of both hydrogen-bonded and free CH_3CN species.[21,25] The free CH_3CN species has the same C≡N stretch frequency as the neat solvent but the H-bonding blue-shifts by ≈6 cm^{-1}.[25−27] When ω_2 is set to 2253 cm^{-1}, the frequency of the free CH_3CN species, there may be a selective enhancement of the free CH_3CN species' combination band at $\omega_1 = 3164$ cm^{-1} and discrimination against the H-bonded CH_3CN species' combination band at higher frequencies. The discrimination results in a narrower line for the DOVE-IR-FWM line than the IR absorption band. This selectivity and line narrowing capability is particularly useful for distinguishing different sites, components, and conformers in complex samples.

To further test the capabilities of DOVE methods for removing spectral congestion, a seven-component $CH_3CN/CD_3CN/CDCl_3/THF/THF\text{-}d_8/C_6D_6/H_2O$ mixture was examined to explore the effect of other absorption and Raman features on the CH_3CN DOVE line. Figures 4a and 4b show the infrared and Raman spectra for the mixture. The infrared spectrum near the ω_2 values in Figure 4a contains lines from the $CDCl_3$ C−D stretch band at 2253 cm^{-1}, the THF-d_8 band at 2240 cm^{-1}, and the 2262 cm^{-1} CD_3CN C≡N stretch that all overlap with the CH_3CN 2253 cm^{-1} line (see the inset of Figure 4a). The infrared spectrum near the ω_1 values of the CH_3CN 3164 cm^{-1} band is nearly buried by the background from the broad O−H stretch band of H_2O, the 3092 cm^{-1} $\nu_2 + \nu_4$ combination band of CD_3CN, and the C−H stretch bands of THF and CH_3CN around 3000 cm^{-1}. Figure 4b shows the Raman spectrum where THF has a ring mode Raman band at 914 cm^{-1} that overlaps with the C−C stretch 918 cm^{-1} Raman band of CH_3CN. The Raman ring mode band of THF-d_8 occurs at 840 cm^{-1} while the CD_3CN C−C stretch Raman band occurs at 832 cm^{-1}. Finally, the C_6D_6 Raman line occurs at 944 cm^{-1}.

To explore the effect of the additional absorption and Raman transitions on the selectivity of DOVE-FWM, the ω_2 laser is set at the 2253 cm^{-1} ν_2 CN stretch of CH_3CN and the ω_1 laser is scanned across the 3164 cm^{-1} $\nu_2 + \nu_4$ combination band of CH_3CN. As we can see from Figure 4c, only the single feature at 3164 cm^{-1} appears in the spectrum. The features of other components are not observed though they appear in the ordinary spontaneous Raman spectrum and the IR absorption spectrum. This spectrum confirms the selectivity of DOVE-FWM methods, their ability to simplify vibrational spectra, and the importance of mode coupling in creating measurable peaks.

Conclusions

This paper has demonstrated the unique selective capabilities of DOVE methods. In particular, the mode selectivity provides the ability to eliminate much of the spectral congestion in complex samples and isolates the features that are coupled by interactions. These capabilities should be particularly important for environmental and biochemical systems where the identification of interacting moieties plays a fundamental role in understanding structure/function relationships. For example, it will be particularly interesting to use DOVE methods for the C═O and N−H stretch modes in proteins because H-bonding interactions will lead to mode coupling that might allow one to identify the interacting moieties,[2,5,15] much as 2D NMR does. The line-narrowing capabilities can also reduce much of the broadening caused by H-bonding interactions while the component selectivity should allow one to isolate particular conformers.

Acknowledgment. This work was supported by the Chemistry Program of the National Science Foundation under grant CHE-9816829.

JA9926414

(25) Jamroz, D.; Stangret, J.; Lindgren, J. *J. Am. Chem. Soc.* **1993**, *115*, 6165−6168.

(26) Jamroz, D.; Wojeik, M.; Lindgren, J.; Stangret, J. *J. Phys. Chem. B* **1997**, *101*, 6758−6762.

(27) Cho, H. G.; Cheong, B. S.; Kim, K. W. *Bull. Korean Chem. Soc.* **1998**, *19*, 909−910.